Author/s:
Thomas, DR;Garnish, SE;Khoo, CA;Padmanabhan, B;Scott, NE;Newton, HJ

Title:
Coxiella burnetii protein CBU2016 supports CCV expansion

Date:
2024-01-01

Citation:
Thomas, D. R., Garnish, S. E., Khoo, C. A., Padmanabhan, B., Scott, N. E. & Newton, H. J. (2024). Coxiella burnetii protein CBU2016 supports CCV expansion. Pathogens and Disease, 82, https://doi.org/10.1093/femspd/ftae018.

Persistent Link:
https://hdl.handle.net/11343/358430

Pathogens and Disease, 2024, **82**, ftae018
DOI: 10.1093/femspd/ftae018
Advance access publication date: 13 August 2024
Research Article

Coxiella burnetii protein CBU2016 supports CCV expansion

David R. Thomas[1,2], Sarah E. Garnish[1], Chen Ai Khoo[1], Bhavna Padmanabhan[2], Nichollas E. Scott[2], Hayley J. Newton[1,2,*]

[1]Infection Program, Monash Biomedicine Discovery Institute and Department of Microbiology, Monash University, Clayton, VIC 3800, Australia
[2]Department of Microbiology and Immunology at the Peter Doherty Institute for Infection and Immunity, University of Melbourne, Melbourne, VIC 3000, Australia
*Corresponding author. Infection Program, Monash Biomedicine Discovery Institute and Department of Microbiology, Monash University, Clayton, VIC 3800, Australia. E-mail: hayley.newton@monash.edu
Editor: [Andrew Olive]

Abstract

Coxiella burnetii is a globally distributed obligate intracellular pathogen. Although often asymptomatic, infections can cause acute Q fever with influenza-like symptoms and/or severe chronic Q fever. *Coxiella burnetii* develops a unique replicative niche within host cells called the *Coxiella*-containing vacuole (CCV), facilitated by the Dot/Icm type IV secretion system translocating a cohort of bacterial effector proteins into the host. The role of some effectors has been elucidated; however, the actions of the majority remain enigmatic and the list of true effectors is disputable. This study examined CBU2016, a unique *C. burnetii* protein previously designated as an effector with a role in infection. We were unable to validate CBU2016 as a translocated effector protein. Employing targeted knock-out and complemented strains, we found that the loss of CBU2016 did not cause a replication defect within Hela, THP-1, J774, or iBMDM cells or in axenic media, nor did it affect the pathogenicity of *C. burnetii* in the *Galleria mellonella* infection model. The absence of CBU2016 did, however, result in a consistent decrease in the size of CCVs in HeLa cells. These results suggest that although CBU2016 may not be a Dot/Icm effector, it is still able to influence the host environment during infection.

Keywords: *Coxiella burnetii*; intracellular bacterial pathogen; replicative vacuole; Dot/Icm secretion system

Introduction

Coxiella burnetii is a globally distributed obligate intracellular pathogen and the causative agent of Q fever. Human infections can present as an acute disease, commonly with influenza-like symptoms, and/or as a chronic infection. Chronic Q fever can arise months to years after infection, often producing severe and potentially fatal endocarditis (Buijs et al. 2021). Indeed, following the large Q-fever outbreak in The Netherlands in 2007, cases of probable and proven chronic Q fever had a 5-year morality rate of 36% (van Roeden et al. 2019). However, ~60% of *C. burnetii* infections are asymptomatic, making infection rates and distribution difficult to ascertain (Maurin and Raoult 1999). In livestock, *C. burnetii* infections can lead to spontaneous abortions and stillbirth, with exposure to bacteria shed from birthing products, faeces, urine, and milk a major source of animal-human transmission (Robi et al. 2023). *Coxiella burnetii* has an extremely wide host range, and so its presence in wildlife near humans and livestock is almost unavoidable. As such, *C. burnetii* is likely to be an ongoing cause of disease requiring the attention of medical research.

Coxiella burnetii infects most cell types but has a tropism for alveolar macrophages (Dragan et al. 2019). Once internalized by the host cell and trafficked through the endocytic pathway, a change in pH and environmental conditions induces a transition from the environmentally stable small cell variant to the metabolically active large cell variant, along with the expression of genes for the Dot/Icm type 4B secretion system (T4SS) and translocation of an estimated 100–150 effector proteins into the host cell (Newton et al. 2013, 2020). These effectors are essential for the development of the spacious *Coxiella*-containing vacuole (CCV), the cellular niche in which the bacteria replicate, and also for host immune evasion (Newton et al. 2014, Burette et al. 2020). The importance of translocated effectors is such that *C. burnetii* mutants lacking a functional T4SS are unable to replicate in host cells (Beare et al. 2011, Carey et al. 2011).

Dot/Icm effector proteins have been predicted computationally and identified from transposon screens looking for obvious defects in replication or CCV development (Chen et al. 2010, Lifshitz et al. 2013, Weber et al. 2013, Newton et al. 2014, Larson et al. 2015). These approaches have successfully identified many key effectors but are not without drawbacks. Due to the time-consuming process of genetically modifying *C. burnetii*, many translocation assays—required to confirm bona fide effectors, have been performed in a surrogate *Legionella pneumophila* system (Chen et al. 2010, Carey et al. 2011, Lifshitz et al. 2013, Weber et al. 2013). While the T4SS of *L. pneumophila* is homologous to that of *C. burnetii*, translocation of *C. burnetii* effectors has not been entirely consistent between the two systems (Larson et al. 2023).

CBU2016 is a putative effector previously identified by a bioinformatic screen (Weber et al. 2013). It first came to our attention as a preliminary hit that failed validation in an infection-based screen (unpublished data). Despite this, its recurrence in the literature and variable reported phenotypes retained our interest. CBU2016 is a highly conserved *C. burnetii* protein, suggesting an important function (Weber et al. 2013). However, as with many

Received 8 January 2024; **revised** 28 July 2024; **accepted** 13 August 2024

novel effectors it is difficult to interrogate *in silico*, with established modelling systems I-TASSER, Phyre2, and AlphaFold unable to identify any protein domains, homologues or predicted structural similarities (Kelley et al. 2015, Yang et al. 2015, Jumper et al. 2021, Varadi et al. 2022). As such, we aimed to confirm the impact of CBU2016 on *C. burnetii* infections and clarify the conflicting reports in the literature.

Translocation of CBU2016 has only been demonstrated via the *L. pneumophila* T4SS using the BlaM translocation reporter assay, and then in only ~1% of infected cells (Weber et al. 2013). In the same publication, Weber et al. reported that a transposon mutant disrupting *cbu2016* did not possess a replicative defect in either HeLa or J774.A1 cells. Martinez et al. (2014), from a separate transposon library, reported a minor replication defect in two CBU2016 transposon mutants during infection of Vero cells, measured using GFP-expressing colony size as a surrogate for bacterial number (Martinez et al. 2014). More recently, Case et al. (2022), using the transposon mutants generated by Weber et al. (2013), found that disruption of *cbu2016* rendered *C. burnetii* unable to replicate in murine bone marrow derived macrophages (BMDM) and suggested a replication defect in J774 cells (Case et al. 2022). The transposon mutant also replicated significantly less in the spleens of severe combined immunodeficiency disease (SCID) mice and induced less splenomegaly than WT *C. burnetii* (Case et al. 2022). However, these studies did not confirm the direct involvement of *cbu2016* through complementation.

To validate the importance of CBU2016 during *C. burnetii* infection, a targeted *cbu2016* deletion mutant and complementation strain were created. Employing these new tools, we found no replication defect in axenic media, in four different mammalian cell lines, nor a change in pathogenicity in the *Galleria mellonella* infection model. However, we did identify a defect in CCV expansion associated with the loss of CBU2016, although accumulation of key markers of endosomal, lysosomal, and autophagosomal fusion were not perturbed by the loss of CBU2016. Finally, we were unable to demonstrate translocation of CBU2016 by *C. burnetii*, indicating that this protein may not be a bona fide substrate of the Dot/Icm secretion system. Given the conservation of the gene in sequenced *C. burnetii* isolates, CBU2016 may be important in defined circumstances not tested here, such as specific host or environmental conditions. This study highlights the importance of confirming translocation in native systems, and employing complemented strains to confidently link phenotypes to genotypes.

Methods

Mammalian cell culture

HeLa (CCL2, ATCC), J774A.1 (ATCC), and iBMDMs (kindly provided by A/Prof Thomas Naderer, Monash University) were cultured in Dulbecco's Modified Eagle's Media with GlutaMAX™ (DMEM, Gibco) supplemented with 10% heat inactivated fetal calf serum (FCS, Gibco). THP-1 cells (ATCC) were cultured in RPMI 1640 (RPMI) supplemented with 10% FCS. Both cell lines were cultured at 37°C, 5% CO_2. For exogenous expression of GFP-tagged proteins, plasmids were transfected into HeLa cells using Lipofectamine 3000 transfection reagent (Invitrogen) according to manufacturer's instructions.

Bacterial cell cultures

Escherichia coli (Pir2) was grown at 37°C in Luria–Bertani broth supplemented with 50 µg/ml Kanamycin or 100 µg/ml ampicillin as required. Plasmids were introduced into Pir2 cells by heat-shock and Sanger sequenced by Australian Genome Research Facility (AGRF). PFU Ultra (Agilent) was used for PCR amplification of DNA fragments and MyTaq™ Red (Bioline) for colony screening.

Coxiella burnetii was grown in ACCM2 at 37°C, 5% CO_2, 2.5% O_2, and supplemented with 3 µg/ml chloramphenicol and/or 350 µg/ml Kanamycin as required (Omsland et al. 2011). The CBU2016 KO strain was created by homologous recombination and sucrose counter-selection as previously to replace *CBU2016* with as kanamycin resistance cassette (Beare and Heinzen 2014). Plasmid DNA was introduced into Coxiella by electroporation and plated onto semi-solid ACCM2 media for screening (Omsland et al. 2011). Liquid cultures of *C. burnetii* were quantified using the PicoGreen Quanti iT™ PicoGreen® dsDNA Assay Kit (ThermoFisher Scientific) or qPCR (SensiFast SYBR No-ROX, Bioline) with oligonucleotides specific for *ompA*, following manufacturer's instructions (Jaton et al. 2013, Newton et al. 2016, Lau et al. 2019). Confirmation of genetic knock-out and complementation was performed on *C. burnetii* bacterial pellets using MyTaq™ Red polymerase according to manufacturer's instructions with primers targeting *cbu2016* (Fwd:AAAACTCGAGGATGGTGGTTATGCTAGAAGACG, Rev: TTTTGGATCCTTAGGGATCGAAGCCGGAGG). Confirmation of 3xFLAG-CBU2016 expression from plasmid was confirmed by western blot. *Coxiella burnetii* cultures were pelleted and resuspended in SDS-lysis buffer at 95°C for 10 min. Lysates were separated on 4%–15% TGX TX Stain-Free™ protein gels (Bio-Rad) and transferred to PVDF membrane using the Trans-blot turbo system (Bio-Rad). Protein blots were blocked in TBS supplemented with 0.1% Tween-20 and 5% skim milk powder (Blocking buffer). Anti-FLAG (Sigma–Aldrich), anti-BlaM (QED Biosciences), and anti-mouse-HRP antibodies were diluted in blocking buffer and incubated on membranes at room-temperature for 1 hour, with 3–5 washes with TBS supplemented with 0.1% Tween-20 (TBS-T) after each incubation. Blots were developed with Clarity Western ECL Reagents (Bio-Rad), and imaged on a Chemidoc Touch (Bio-Rad). Protein loading was confirmed by stain-free imaging.

Infection of mammalian cells with *C. burnetii*

Intracellular replication was measured using established protocols (Newton et al. 2016, Lau et al. 2019, Loterio et al. 2023). Briefly, HeLa and J774 cells were seeded into 24 well plates at 2×10^4 cells per well the day before infection, and iBMDMs the day before infection at 0.5×10^4 cells per well. THP-1 cells were seeded at 5×10^5 cells per well and differentiated with 10 nM phorbol 12-myristate 13-acetate (PMA, Adipogen Life Sciences) three days prior to infection. To infect cells, 7-day axenic cultures of *C. burnetii* were resuspended in RPMI + 5% FCS to infect THP-1 cells or DMEM + 5% FCS for other cell lines. Bacteria were quantified and added to cells at the indicated MOI in 500 µl. Plates were spun at 500 g for 30 min at 30°C, then washed once with PBS and once with DMEM or RPMI (for HeLa, J774, and iBMDMs, or THP-1s, respectively) + 5% FCS, and left in 500 µl fresh media + 5% FCS at 37°C, 5% CO_2. Four days post infection, an additional 250 µl of media + 5% FCS was added to cells. At indicated times post infection, cells were lysed with distilled water and bacteria were pelleted from the lysates and growth media by centrifugation. DNA was extracted from samples using the Quick DNA MiniPrep Kit (Zymo Research) and quantified by qPCR as above. For immunofluorescence assays, infection of HeLa cells was performed as above, but cells were seeded on #1.5 12 mm round coverslips. Infection of

THP-1 s for translocation assays were performed in 96-well, clear bottomed black walled plates (Perkin Elmer). Cells were seeded and differentiated for three days prior to infection with *C. burnetii* at an MOI of 100 as above, but media was not replaced after centrifugation. After 24 h, translocation was assessed using the LiveBLAzer™ FRET-B/G Loading Kit with CCF2-AM (ThermoFisher) following manufacturer's instructions. After incubation at room temperature for two hours, fluorescence was measured on a a CLARIOstar® Plus plate reader (BMG LABTECH) and imaged using a Leica Thunder Deconvolution microscope with 10× objective. Images were analyzed using CellProfiler (Stirling et al. 2021).

Immunofluorescence

HeLa cells were fixed with 4% PFA paraformaldehyde (PFA) for 15 min, washed three times with PBS, then permeabilized with PBS + 1% bovine serum albumin (BSA, Roche) and 0.2% Triton X-100 for 15 min. Cells were washed with PBS and blocked for at least 1 h in PBS + 0.1% Tween-20® and 1% BSA (blocking buffer). All primary (rabbit anti-*C-burnetii* [in house], Mouse anti- LAMP1 [Developmental Studies Hybridoma Bank], Mouse anti- GFP [ThermoFisher]) and secondary (Goat anti- Mouse488 and Goat anti-rabbit647, ThermoFisher) antibodies were diluted in blocking buffer, and incubated for 1 h at room temperature, with three TBS-T washes between primary and secondary incubations (Carey et al. 2011). Coverslips were stained with 4,6-diamidino-2-phenylindole (DAPI, Life Technologies) before five additional washes in TBS-T and mounting with ProLong Gold (Life Technologies). Samples were imaged on Zeiss LSM700 and Leica SP8 invert confocal microscope with 63× oil-immersion objectives. Images were analyzed using FIJI (Schindelin et al. 2012). To quantify marker accumulation at CCVs, fluorescence intensity measurements within the CCV (for LC3) or a 3-pixel wide line containing the CCV membrane (for Lamp1, Rab7, and clathrin) were compared to intensity measurements from an adjacent cytoplasmic region. Background fluorescence from a cell-free region of the image was subtracted from all measurements.

Galleria mellonella infections

Galleria mellonella colonies were maintained in-house at 30°C in the dark until use, and infections were performed as previously (Norville et al. 2014, Kuba et al. 2020). Briefly, *C. burnetii* was resuspended in PBS to a concentration of 1×10^8 GE/ml, and 10 µl injected into the uppermost proleg of *G. mellonella*. Following infection, larvae were isolated in 12-well tissue cultures plates and kept in the dark at 37°C. Survival was assessed every 24 h for 10 days.

Sample preparation for mass spectrometry

To examine changes to the host proteome during infection, HeLa cells in 10 cm dishes were infected with *C. burnetii* at an MOI of 100 in 5% DMEM, or left uninfected, for 3 days. Before harvesting, cells were observed to confirm consistent infection levels across strains and replicates, which were estimated to be >90% for all groups. To harvest, cells were washed with ice cold PBS and resuspended in 500 µl of lysis buffer (50 mM Tris.HCl [pH 8], 5% SDS, and 1× protease inhibitor; Roche) before shaking at 95°C and 1500 RPM to 10 min to shear DNA. Protein content in samples was quantified using a BCA kit (Pierce) following the manufactures instructions. S-Trap™ Micro spin columns (ProtiFi) were used to prepare 100 µg of protein from each sample according to manufacturer's instructions. Briefly, samples were reduced by the addition of 20 mM Dithiothreitol (DTT) and boiling at 95°C for 10 min then alkylated by the addition of 40 mM iodoacetamide for 30 min at room temperature in the dark. Samples were quenched by the addition of another 20 mM DTT, and acidified by the addition of aqueous phosphoric acid to 1.2%. A 6:1 ratio of wash buffer (100 mM Tris–HCl pH 7.5, 90% methanol) was then added to each sample and run though S-Trap™ Micro spin columns. Columns were washed four times with 150 µl of wash buffer, then bound proteins digested overnight with 3 µg of Sequencing Grade Modified Trypsin (Promega). Peptides were eluted as per protocol, dried down in a spin vacuum, and resuspended in buffer A* (0.1% trifluoroacetic acid, 2% acetonitrile) for analysis.

For proteomic analysis of axenic *C. burnetii* cultures, 7-day cultures were collected by centrifugation and quantified by BCA assay. Bacterial pellets containing 200 µg of protein were resuspended in 25 µl of bacterial lysis buffer (50 mM Tris–HCl [pH 8], 5% SDS, 1% Triton X-100, 0.25% NP-40 substitute, 1 mM $MgCl_2$, 125 U/ml benzonase, 1× protease inhibitor) before shaking at 95°C and 1500RPM to 10 min to shear DNA. Samples were then prepared for digestion on S-Trap™ Micro spin columns as above. Dried samples were submitted to further purification using C18 Stage tips to remove particulate matter (Rappsilber et al. 2003, Rappsilber et al. 2007).

Reverse phase liquid chromatography-mass spectrometry

Prepared purified peptides from each sample were re-suspended in Buffer A* and separated using a two-column chromatography setup composed of a PepMap100 C_{18} 20-mm by 75-µm trap and a PepMap C_{18} 500-mm by 75-µm analytical column (Thermo Fisher Scientific). Samples were concentrated onto the trap column at 5 µl/min for 5 min with Buffer A (0.1% formic acid, 2% DMSO) and then infused into an Orbitrap Q-Exactive plus (Thermo Fisher Scientific) at 300 nl/min via the analytical columns using a Dionex Ultimate 3000 UPLC (Thermo Fisher Scientific). Samples were separated using a 125-min analytical gradient undertaken by altering the buffer composition from 2% Buffer B (0.1% formic acid, 77.9% acetonitrile, 2% DMSO) to 22% B over 95 min, then from 22% B to 40% B over 10 min, then from 40% B to 80% B over 5 min. The composition was held at 80% B for 5 min, and then dropped to 2% B over 1 min before being held at 2% B for another 9 min. The Orbitrap QE plus mass spectrometer was operated in a data-dependent mode automatically switching between the acquisition of a single Orbitrap MS scan (375-1400 m/z and a resolution of 70k) and 15 Orbitrap MS/MS HCD scans of precursors (Stepped NCE of 28;30 and 32%, an Automatic Gain Control (AGC) value of 2e3 and maximal injection time of 50 or 110 ms using either resolution of 17.5k or 35k, respectively).

Proteomic data analysis

Identification of peptides was accomplished with FragPipe (V20.0) using the Open Search workflow for infected mammalian cells, and the LFQ-MBR workflow for axenic *C. burnetii* (Kong et al. 2017). Data was searched against the human (Uniprot: UP000005640) or *C. burnetii* (Uniprot: UP000002671) proteome. The resulting Top-N data were processed using Perseus (V2.0.3.0) (Tyanova et al. 2016). For comparisons, biological replicates were grouped and proteins filtered to include only those with at least three values in any group. Missing values were imputed based on total peptide intensities using a range of 0.3σ and downshift of 2.3σ. Proteomes were compared with Student's *t*-tests corrected for multiple comparisons using Benjamini–Hochberg correction at an FDR of 0.05 and

S0 of 0.1 or by ANOVA with FDR limited to 0.05 and S0 of 0. Data were exported and visualized using Graphpad Prism. Proteomics data have been deposited to the PRIDE partner repository with the data set identifier PXD047783 and can be accessed using the username: reviewer_pxd047783@ebi.ac.uk and password: YJaoEz6P.

Statistical analysis

Unless otherwise stated, data were analyzed using GraphPad Prism 10 software. Data are presented throughout as mean ± standard deviation, and differences were considered statistically significant when P was < 0.05 as indicated in the figures.

Results

CBU2016 is not required for replication of *Coxiella burnetii*

To examine the function of CBU2016 in the biology of *C. burnetii*, a knock-out (KO) mutant was generated by replacing *cbu2016* in *C. burnetii* Nine Mile II (RSA439, phase II, clone 4, WT) with a kanamycin resistance cassette as previously described (Beare and Heinzen 2014). The *cbu2016* knock-out mutant (Δ*cbu2016*) was then complimented with a plasmid encoding for 3xFLAG-tagged CBU2016 under the control of the P1169 constitutive promoter (Δ*cbu2016*:FLAG2016) (Voth et al. 2011). The success of the KO and complementation was confirmed by PCR and western blotting (Fig. S1A and B). Seven-day old cultures of *C. burnetii* WT, Δ*cbu2016*, and Δ*cbu2016*:FLAG2016 were quantified and used to seed new ACCM2 cultures at a starting density of 10^6 genomic equivalents (GE)/ml. Samples were taken daily and GE quantified to track bacterial replication. After 7 days, there was no significant difference between the growth curves of the three strains ($P = 0.154$), with all strains entering stationary phase at approximately day five (Fig. 1a). We next sought to confirm whether the absence of *cbu2016* led to an intracellular replication defect. HeLa and THP-1 cells were infected with *C. burnetii* WT, Δ*cbu2016*, or Δ*cbu2016*:FLAG2016 at MOIs of five and 2.5, respectively. Cells were harvested immediately after infection (day 0), and 1-, 3-, and 5-days post infection for quantification. In both cell types, significant replication was observed at 3 days post infection, but no significant differences were detected between the three strains at any time point (Fig. 1b and c). To attempt to replicate defects in cell lines reported in the literature, we also assessed replication curves in J774 and immortalized mouse-derived bone marrow derived macrophages (iBMDMs). As with HeLa and THP-1 s, extensive intracellular replication was detected 3- and 5-days post infection, but no difference in replication between the strains was observed in either iBMDMs or J774s (Fig. 1d and e).

CBU2016 does not influence pathogenicity in *Galleria mellonella*

The observation by Case et al. (2022) that a CBU2016 transposon mutant is less pathogenic in the SCID mouse model of infection indicated that this protein may aid in resisting the innate immune response, given SCID mice lack functional adaptive immunity (Case et al. 2022). *Galleria mellonella* (wax moth larvae) have been used as an infectious model for ∼65 pathogens and are a valuable model for *C. burnetii* infections due to their susceptibility to the attenuated Phase II strain and possession of innate immune responses homologous that that of mammals (Norville et al. 2014, Asai et al. 2023). Importantly, the *G. mellonella* model was able to detect changes in the virulence of CBU1543 (MceF) and CBU0021 (Cig2/CvpB) transposon mutants, despite the absence of these T4SS effectors not causing a replication defect in cell culture (Newton et al. 2014, Kohler et al. 2016, Loterio et al. 2023). To explore a potential role for CBU2016 in pathogenicity *in vivo*, *C. burnetii* WT, Δ*cbu2016*, and Δ*cbu2016*:FLAG2016 were injected into *G. mellonella* larvae and survival was tracked over 10 days. However, as with intracellular replication, no significant change in pathogenicity was detected between any of the *C. burnetii* strains ($P > 0.05$, Mantel–Cox test, Fig. 1f).

CBU2016 supports CCV expansion

A significant number of *C. burnetii* Dot/Icm effectors are involved in the development and/or maintenance of the CCV, and so we next considered if CBU2016 had a similar role. HeLa cells were infected with *C. burnetii* WT, Δ*cbu2016*, and Δ*cbu2016*:FLAG2016 at an MOI of 50 for 3 days. Cells were then fixed and immunostained for *C. burnetii* and LAMP-1, a lysosomal marker that also accumulates at the CCV membrane. Interestingly, compared to WT, a statistically significant average decrease of 31.6 ± 12.9% ($P < 0.001$) in CCV size was observed from infections with Δ*cbu2016*; a phenotype that was recovered by complementation in Δ*cbu2016*:FLAG2016 (Fig. 2a and c). There was also a small but statistically significant decrease of 6.5 ± 8.1% ($P = 0.014$) in the proportion of infected cells containing a single CCV in Δ*cbu2016* infections compared to WT (Fig. 2a and c). However, data from the Δ*cbu2016*:FLAG2016 complemented strain were consistent with the KO strain, suggesting the slight difference in CCV number is not dependent on CBU2016.

CBU2016 is not required for vesicle-CCV fusion

Coxiella burnetii co-opts various cellular trafficking systems to facilitate CCV expansion. As a result of vesicle fusion, key host proteins become localized to the CCV membrane. To assess if the defect in CCV expansion was due to altered vesicle trafficking to the CCV in the absence of CBU2016, the localization of several markers was measured. In addition to examining endogenous LAMP1, GFP fusion proteins of Rab7 (mouse), clathrin (rat, light chain), and LC3B were transfected into HeLa cells infected with *C. burnetii* WT, Δ*cbu2016*, and Δ*cbu2016*:FLAG2016. The ratio of fluorescence at the CCV compared to the cytoplasm was then measured after 3 days. Rab7 is a marker of endosomes found to associate at the CCV membrane, and its disruption has been shown the decrease CCV size (Beron et al. 2002). Similarly, clathrin is involved in endocytosis and cellular trafficking, and its absence also results in reduced CCV expansion (Larson et al. 2013, Latomanski et al. 2016). LC3 is an essential protein involved in autophagosome biogenesis that accumulates at the CCV, and when prevented from doing so also results in defective CCV biogenesis (Newton et al. 2014). After 3 days of infection, there was no significant difference in the distributions of Rab7 (Fig. 3a), LC3 (Fig. 3b), Clathrin (Fig. 3c), or LAMP-1 (Fig. 2c and d) amongst the three *C. burnetii* strains. All of the examined host proteins accumulated at the CCV membrane (or within the CCV for LC3), indicating that the successful fusion of late endosomes, clathrin coated vesicles, autophagosomes, and lysosomes is not reliant on CBU2016.

Dot/Icm translocation of CBU2016 by *C. burnetii* could not be observed

Although previously shown to be translocated by the *L. pneumophila* T4SS (Weber et al. 2013), we sought to confirm if CBU2016 was indeed translocated by the *C. burnetii* Dot/Icm system. *C. burnetii* WT and the Dot/Icm deficient transposon mutant *icmL*::Tn

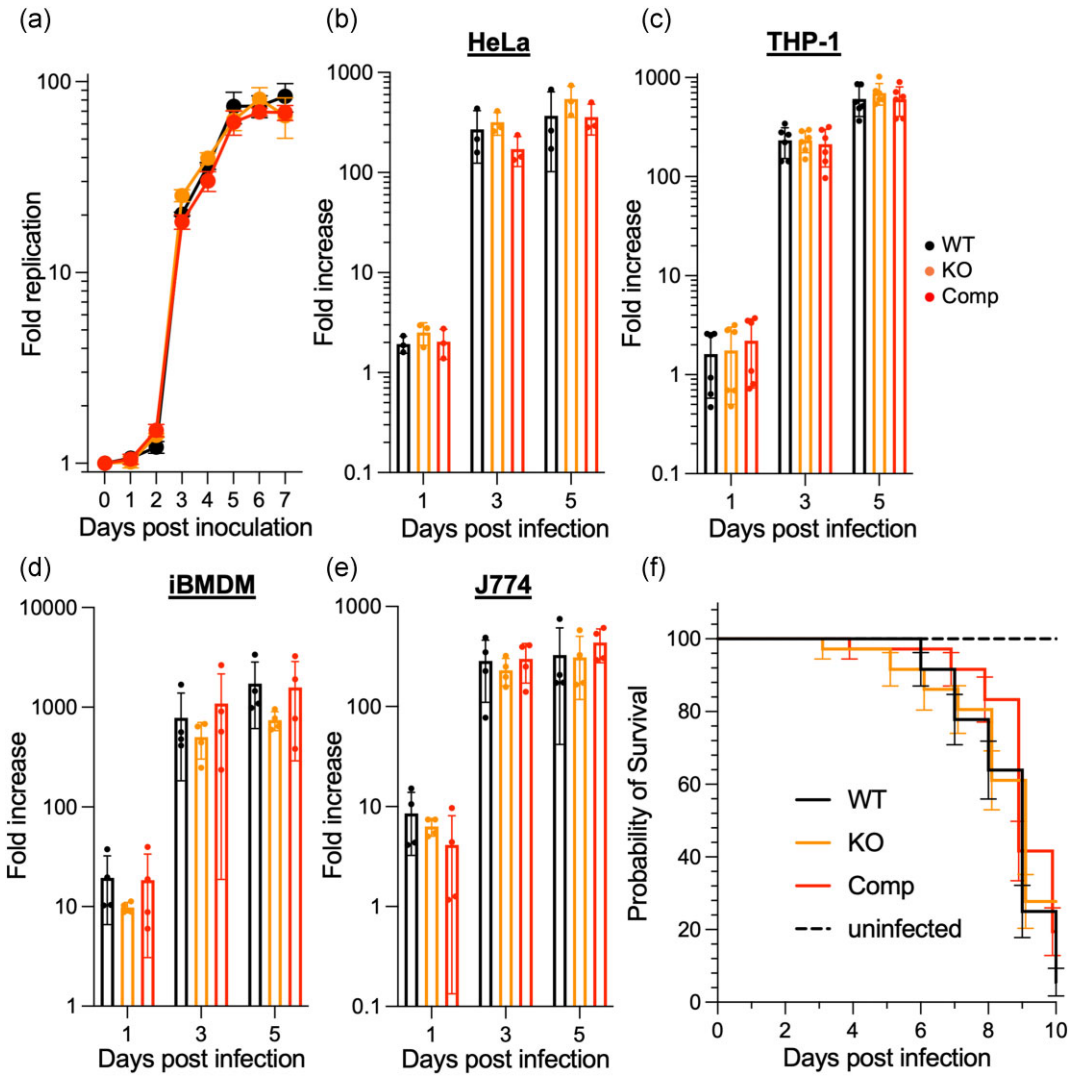

Figure 1. CBU2016 does not impact *Coxiella* replication. (a) *C. burnetii* WT (black), Δ*CBU2016* (KO, orange), and Δ*CBU2016*:FLAG2016 (Comp, red) strains were seeded into ACCM2 and measured every 24 h for 7 days. Replication is given as fold change in GE from day 0. (b-c) HeLa (b), THP-1 (c), iBMDM (d), and J774 (e) cells were infected with *C. burnetii* at an MOI of five for HeLa, and 2.5 for all others. DNA was extracted and GE measured by qPCR immediately (zero), 1-, 3-, and 5-days post infection. GE quantities are presented as fold increase from D0 values. Graphs shown are mean ± SD of three (a, b), four (d, e), or six (c) independent experiments. (f) *Galleria mellonella* larvae were injected with 1×10^6 GE of WT, Δ*CBU2016*, and Δ*CBU2016*:FLAG2016 (Comp) *C. burnetii* diluted in PBS, or PBS alone (uninfected), and survival was tracked over 10 days. Data represent mean ± SEM of larvae from three independent experiments, with 12 larvae per group. Statistical analysis of a by Extra sum-of-squares test, and b–e by two-way ANOVA with Dunnett's multiple comparison test. Statistical analysis of F by Log-rank (Mantel–Cox) test.

were transformed to express CBU2016 and MceA (CBU0077), an established positive control, N-terminally fused to beta-lactamase (BlaM) (Carey et al. 2011, Fielden et al. 2017). The expression of fusion proteins by *C. burnetii* was confirmed by western blotting (Fig. S2). THP-1 cells were infected with these strain for 24 hours, then CCF2-AM (LiveBLAzer kit) was added for a further two hours. Translocation, represented by a shift from green (450 nm) to blue (520 nm) fluorescence through BlaM-mediated cleavage of the CCF2 substrate, was then measured on a plate reader and by fluorescence microscopy. As expected, a strong shift in the blue/green ratio was observed in cells infected with *C. burnetii* expressing BlaM-MceA, while fluorescence from cells infected with *C. burnetii icmL*::Tn expressing BlaM-MceA was consistent with that of uninfected cells (Fig. 4a). This result was confirmed by microscopy, which found an average of 31.3 ± 0.88% of cells infected with *C. burnetii* WT were positive for BlaM-MceA translocation, while no *C. burnetii icmL*::Tn infected cells gave a positive signal (0.08 ± 0.07%, Fig. 4b and c). In contrast, there was no significant difference in fluorescent ratios of THP-1 cells infected with WT or *icmL*::Tn strains expressing BlaM-CBU2016 when measured by fluorescence plate reader, and both strains produced translocation positive signals in fewer than 0.1% of cells when assessed by microscopy (Fig. 4a, b, and c). Despite showing that CBU2016 influences CCV expansion, this study has been unable to demonstrate that CBU2016 is a substrate of the *C. burnetii* Dot/Icm T4SS.

Loss of CBU2016 does not alter the host proteome during infection

To determine if the loss of CBU2016 alters the proteome of infected cells, we used quantitative label-free proteomics. HeLa cells infected with *C. burnetii* WT or Δ*cbu2016* strains for three

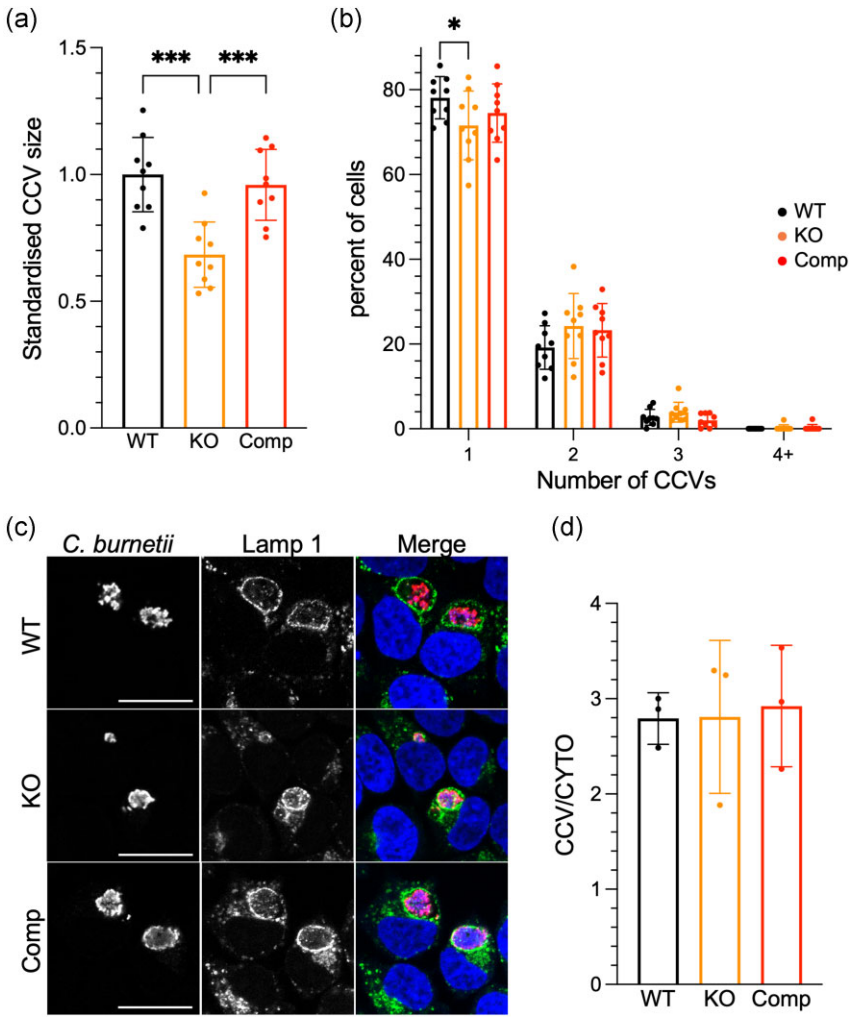

Figure 2. CBU2016 supports CCV expansion. HeLa cells were infected with *C. burnetii* WT (black), Δ*CBU2016* (KO, orange), and Δ*CBU2016*:FLAG2016 (Comp, red) at an MOI of 50 for 3 days before fixing and immunostaining for Lysosomal-associated membrane protein 1 (Lamp1) and *C. burnetii* and imaging by confocal microscopy. CCV size (a) and number per cell (b) was measured using FIJI. CCV size was standardized to mean WT values. (c) representative figures of those used for quantification in a, b, and d. d) Ratios of Lamp1 fluorescence intensity at the CCV membrane compared to the cytoplasm (CCV/CYTO). Scale bar = 20 μM. Data in a and b represent mean ± SD of nine independent experiments, with at least 40 infected cells per condition, while d represents mean ± SD of three independent experiments, with at least 30 infected cells per condition. Statistical analysis of a and d by one-way ANOVA with Tukey's multiple comparison test, and b by two-way ANOVA with Tukey's multiple comparison test. NS = not significant, *$P < 0.05$; ***$P < 0.001$.

days were harvested alongside uninfected cells, in quadruplicate, and processed for analysis by mass spectrometry (MS). Given the defect in CCV expansion was observed at three days post infection, this same timepoint was chosen for proteomic analysis. Across replicates, 5822 human proteins were detected, of which 4115 met the threshold for analysis (proteins observed in at least three biological replicates of one biological group). There were no significant differences in the HeLa proteome between samples infected with WT or Δ*cbu2016* strains (Fig. 5a), and differentially expressed proteins between uninfected, WT, and Δ*cbu2016* infections shows a clear contrast between infected and uninfected samples (Fig. 5b). Two proteins did appear to differ (despite not reaching statistical significance) between infections (EEF1E1 and ANKRD20A4P, Fig. 5a). However, no more than a single peptide spectra was detected in any sample for either protein and variation was driven by imputed values. As such, they were not considered for further analysis.

A similar approach was taken to compare the proteomes of seven-day axenic cultures of *C. burnetiid* WT or Δ*cbu2016* in quadruplicate. Of 1303 proteins identified, 1244 met the threshold for analysis (proteins observed in at least three biological replicates of one biological group), none of which were significantly different between WT or Δ*cbu2016* strains (Fig. 5c). It should be noted that CBU2016 is natively present in low abundance and statistical significance was not reached for this protein due to limitations associated with imputed values: a well-known problem for proteomics (Kong et al. 2022, Vanderaa and Gatto 2023). However, examination of the unimputed CBU2016 intensities confirmed its absence in Δ*cbu2016* samples (Fig. 5d). *Coxiella burnetii* protein CBU1084 (Fig. 5c) was also approaching statistical significance, at levels approximately 2-fold higher in the Δ*cbu2016* strains than in WT. CBU1084, also known as *gacS.3*, has been annotated as an orphan histidine kinase, with no identified substrate (Wachter et al. 2023). While sgRNA silencing of *gacS.3* did not reduce intracellular replication in Vero cells, a TraDIS screen did identify it as a gene

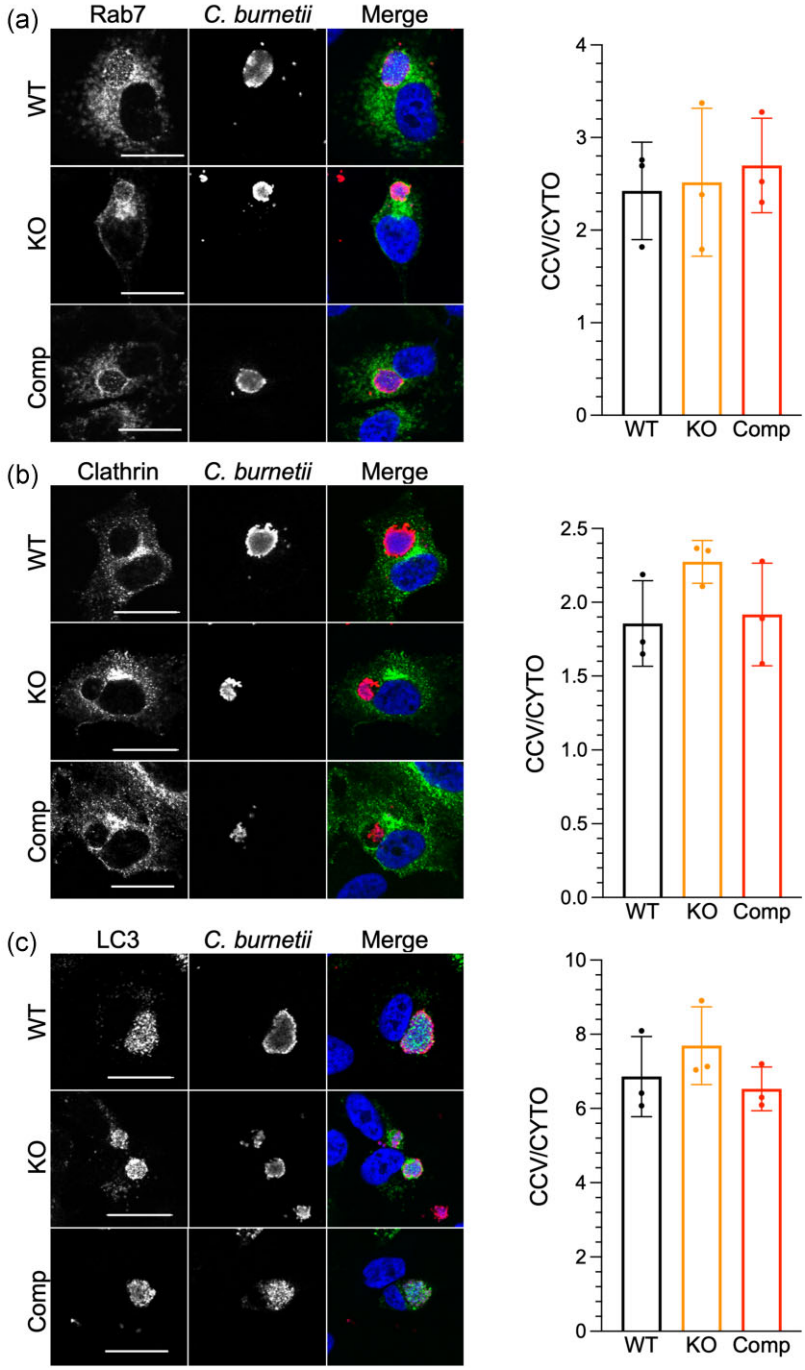

Figure 3. CBU2016 is not required for vesicle fusion with CCVs. HeLa cells were transfected with plasmids to express GFP-tagged mouse Rab7 (a), LC3B (b), or Clathrin (c, rat light chain) and infected with *C. burnetii* WT, Δ*CBU2016* (KO), and Δ*CBU2016*:FLAG2016 (Comp) at an MOI of 50 for 3 days. Cells were fixed and immunostained for GFP and *C. burnetii* and imaging by confocal microscopy. Graphs show ratios of marker fluorescence intensity at the CCV membrane (Rab7 and clathrin) or within the CCV (LC3), compared to the cytoplasm (CCV/CYTO). Scale bar = 20 μM. Data graphs represent mean ± SD of three independent experiments, with at least 20 infected cells per condition. Statistical analysis by one-way ANOVA with Tukey's multiple comparison test.

essential for replication in ACCM2, making its potential upregulation in the Δ*cbu2016* difficult to interpret (Metters et al. 2023). Another protein, Cbu2040 (Fig. 5c), also appeared strongly (but not statistically significantly) altered. However, as above, this difference was attributable to imputed values used in place of missing data. Taken together, this proteomic analysis does not provide any further insight into the role of CBU2016 during *C. burnetii* infection.

Discussion

This study examined the role of CBU2016, a highly conserved *C. burnetii* protein previously designated as a T4SS effector. Using a deletion mutant and complemented strain, we found that the loss of CBU2016 did not reduce the ability of *C. burnetii* to replicate in either axenic ACCM2 media or in HeLa, THP-1, J774, and iBMDM cells. We also did not detect a change in the host cell pro-

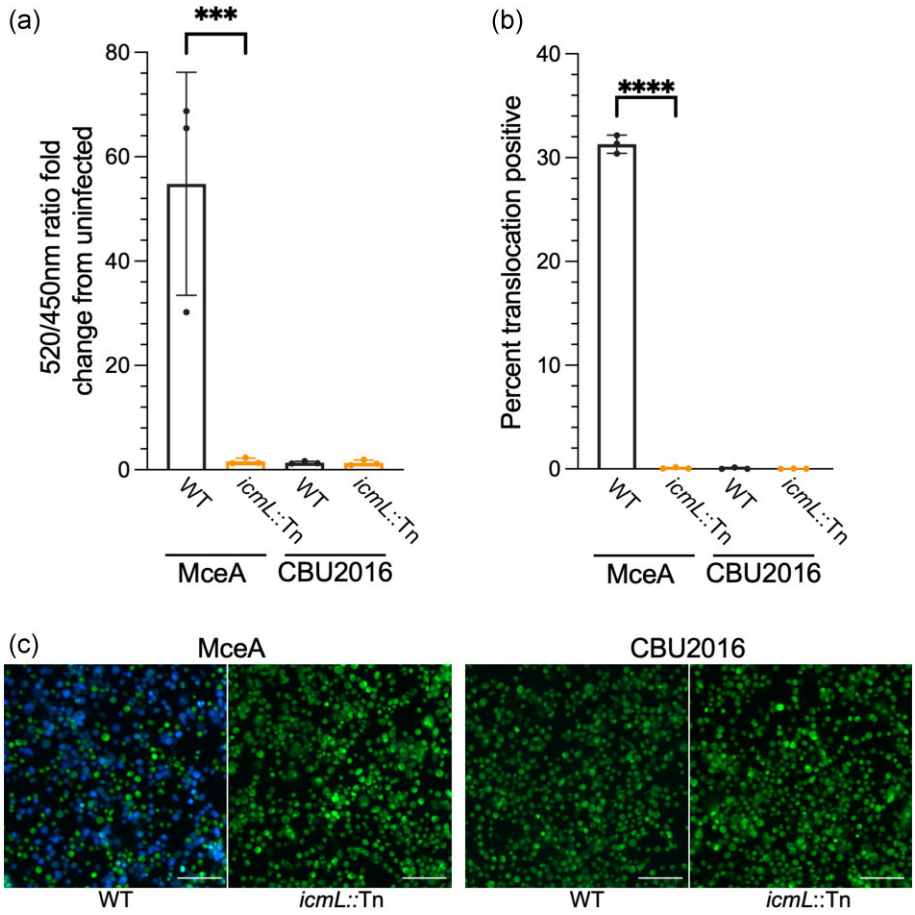

Figure 4. CBU2016 translocation is not observed via reporter assay. *C. burnetii* WT or *icmL*::Tn (T4SS deficient) expressing BlaM fused to either MceA or CBU2016 was used to infect THP-1 cells at an MOI of 100 for 24 h before the addition of the Beta lactamase substrate CCF2-AM. Effector translocation resulted in a shift in CCF2 fluorescence from 520 nm to 450 nm. (a) 450/520 ratio relative to uninfected cell as measured on plate reader. (b) Proportion of translocation positive cells detected by fluorescence microscopy. Cells were analyzed using CellProfiler and considered positive if the signal from cleaved CCF2 was 3-fold above background. (c) Representative figures of those used for quantification in b. Data represent mean ± SD of three independent experiments, with at least 16 000 infected cells per treatment assessed for b. Statistical analysis by one-way ANOVA with Šídák's multiple comparisons test. NS = not significant, ***$P < 0.001$, ****$P < 0.0001$. Scale bar = 100 µM.

teome during infection with either *C. burnetii* WT or Δ*cbu2016*, nor in the proteomes of the axenically cultivated strains. As with any proteomic experiment, it is possible that protein abundance changes may have been missed if they occurred below the limit of detection. Similarly, taking this snapshot approach may have missed differences that occur earlier in infection. We did, however, identify that the loss of CBU2016 leads to a significant decrease in the size of CCVs during infection of HeLa cells: a phenotype which was recovered by complementation. Key markers of vesicle fusion still accumulated at *C. burnetii* Δ*cbu2016* CCVs, indicating that the delivery of lysosomes, endosomes, autophagosomes, and clathrin coated vesicles to the developing CCV was still occurring.

Analysis of CBU2016 translocation in THP-1 cells using the established BlaM/CCF2-AM system failed to detect any translocation of the BlaM-CBU2016 fusion protein. We are careful to note that a lack of detection cannot conclusively confirm a lack of translocation, but instead could be due to other factors. It is possible that CBU2016 is rapidly degraded once translocated into the host cell, or sequestered in sub-cellular compartments where CCF2 is not as readily available. Alternatively, translocation of CBU2016 may be restricted to specific times or environmental conditions, which may have fallen outside the systems we employed. An additional caveat to using this reporter assay is the requirement to examine translocation of a fusion protein. BlaM is 29 kDa with the potential to influence the ability of an effector to be transported through a T4SS apparatus, although prior studies have demonstrated low efficiency translocation of BlaM-CBU2016 in *L. pneumophila* (Weber et al. 2013). A recent study indicates that effector translocation in *L. pneumophila* does not necessarily reflect translocation in *C. burnetii*: in an assessment of 27 effectors translocated by *L. pneumophila* in the literature, only three were detectably translocated by *C. burnetii* (Larson et al. 2023). Regardless of translocation status, the loss of CBU2016 did result in a change in CCV development during infection.

Similar outcomes, including smaller CCVs but no reduction in bacterial replication, have been observed in the *C. burnetii* literature. Interestingly, phenotypes disconnecting CCV size and bacterial replication are often induced as a result of defects in host autophagy. For example, silencing of the autophagy master regulators, TFEB and TFE3, or knocking out the autophagy protein ATG16L1, significantly reduced the size of CCVs, while having no effect on *C. burnetii* replication, while other studies have found that TFE3/TFEB knockout cells can actually support higher levels of bacterial replication in significantly smaller CCVs (Larson et al. 2019, Padmanabhan et al. 2020, Lau et al. 2022). Inversely,

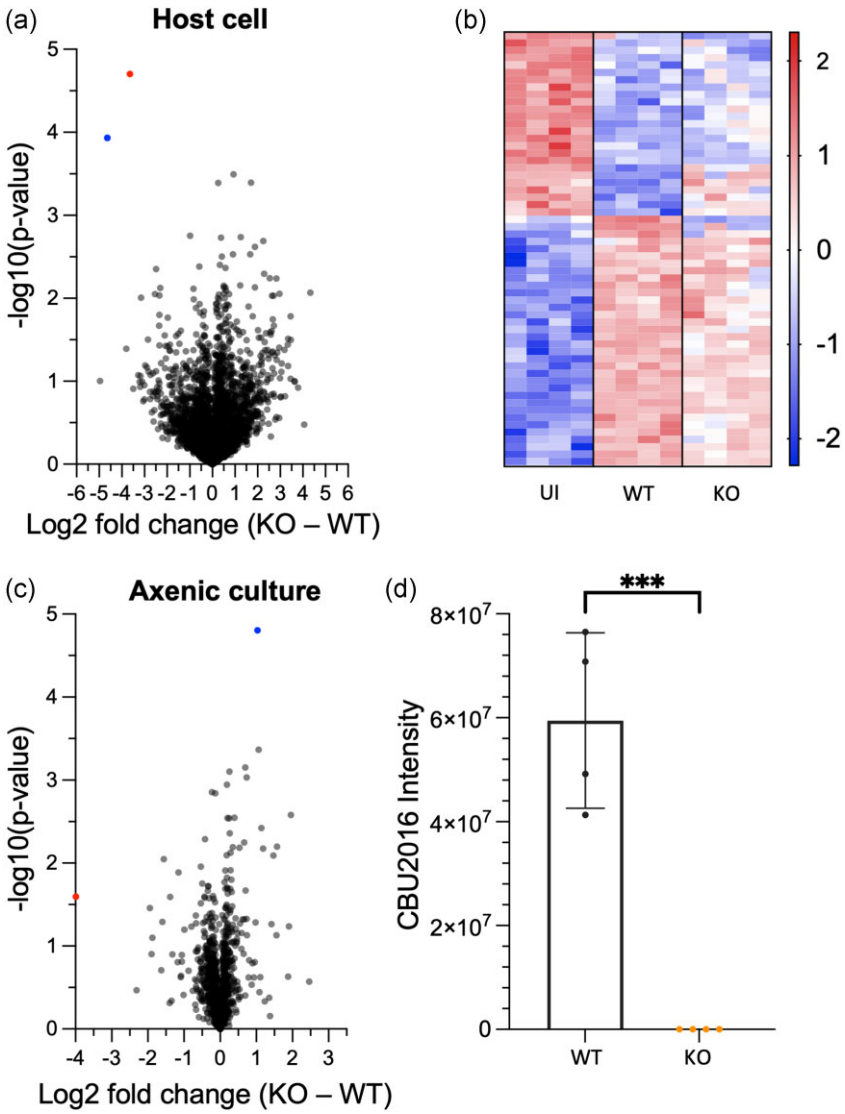

Figure 5. Loss of CBU2016 does not alter the host proteome during infection. HeLa cells were left uninfected or infected with *C. burnetii* WT or Δ*CBU2016* (KO) at an MOI of 100 for 3 days before samples were lysed and analyzed by MS. (a) Volcano plot comparing human proteins identified in samples infected with *C. burnetii* WT or KO. Red: ANKRD20A4P, blue; EEF1E1 (b) z-scored values of proteins differentially expressed between uninfected, WT, and KO infected HeLa cells. (c) Volcano plot comparing proteins identified from *C. burnetii* WT or KO cultures. Red: CBU2040, blue; CBU1084 (d) Comparison of raw, unimputed intensity values of CBU2016 detected in axenic *C. burnetii* WT and KO. Each experiment consisted of four biological replicates. Curves in a and c indicate the threshold for significance determined by Perseus, using Student's *t*-tests with FDR of 0.05 and S0 of 0.1. Proteins in b were identified by ANOVA with FDR limited to 0.05 and S0 of 0. Statistical analysis of d by Student's *t*-test, ***$P < 0.001$, data represent mean ± SD of four biological replicates.

induction of autophagy has be shown to increase CCV size but not replication, while overexpression of TFEB decreased both CCV size and bacterial replication (Latomanski and Newton 2018, Larson et al. 2019, Samanta et al. 2019). However, strong interventions targeting autophagy, such as treatment with 3-MA or silencing/knocking out autophagy proteins AGT16L1, ATG5, or ATG7, are also associated with a significant increase in the number of CCVs per cell (Martinez et al. 2016, Latomanski and Newton 2018, Lau et al. 2022). While a decrease in the proportion of cells with only a single CCV was observed in Δ*cbu2016* infections, the decrease compared to WT (71.6 ± 8.1% vs 78.1 ± 5.0%) was minimal. This may indicate that if CBU2016 modulates autophagy, it is restricted to a fine-tuning/niche activity, or that there is redundancy with other *C. burnetii* proteins performing similar tasks. Alternatively, our data may imply that rather than a CCV fusion or expansion defect, the absence of CBU2016 may increase lysosomal reformation or CCV fission.

While these examples indicate host processes that influence CCV biogenesis, absence of the *C. burnetii* T4SS effector CBU2028 also leads to a similar phenotype to the Δ*cbu2016* strain. *CBU2028*::Tn infections of HeLa cells produced significantly smaller CCVs than WT but were not defective in intracellular replication (Crabill et al. 2018). However, as with CBU2016, Dot/Icm-dependent translocation of CBU2028 has only been confirmed in *L. pneumophila* at a rate of 1% (Weber et al. 2013).

Employing our deletion and compliment strains, our data is in agreement with reports from Weber et al. (2013) who found no replication defect in HeLa or J774 cells, and Martinez et al. (2014) who detected decreased colony size (comparable to CCV size here) in two transposon mutants in Vero cells (Weber et al. 2013, Mar-

tinez et al. 2014). However, our data differs from Case et al. (2022) who detected a decrease in replication in J774 cells, and a complete inability to replicate in BMDMs (Case et al. 2022). The reasons for this divergence could be due to the specific background of the mammalian cells used for infections. Additionally, the comparison is between transposon mutants and the targeted gene deletion strain used here, so variations may also arise from the bacterium. The long periods of axenic culture required for the creation of *C. burnetii* mutants may facilitate the undetected accumulation of mutations that impair intracellular replication, and so could provide an explanation for differing phenotypic outcomes, highlighting the value of complementing knockout strains where possible.

As Dot/Icm-dependent translocation of CBU2016 was not detected, this protein potentially supports CCV development via indirect methods. It may support the translocation of other effectors or their post-translational modification. It may also be involved in nutrient acquisition or metabolite production. The experimental systems we use are largely nutrient replete, and so could potentially obscure phenotypes if CBU2016 is functional under starvation conditions or in response to the depletion of key elements. It is also an important factor that the effect of nutrient restriction on *C. burnetii* replication varies with cell type, and so an effect of CBU2016 may require a specific combination of cell and environment to be detectable (Sanchez et al. 2021). Interactions between cell type and nutrient availability may also explain some of the variability in CBU2016 outcomes in the literature, including the lack of phenotype in our *G. mellonella* model compared to the strong attenuation in SCID mice.

There is significant complexity in native *C. burnetii* infections that cannot be captured in standard experimental models. This includes variations in the nutrient content and cellular composition of diverse tissue types within an organism, and how that might change in response to infection. Future work into CBU2016, and potentially CBU2028, should consider interactions between cell type and nutrient availability on bacterial replication. Differences may become apparent in the ability of *C. burnetii* to import, export, utilize, or detoxify key metabolites that are important when infecting a subset of cell or tissue types. It is possible that there are multiple *C. burnetii* proteins which are advantageous for survival under conditions found within a host during infection, but absent from simplified *in vitro* systems. While this study is unable to identify a specific activity of CBU2016, we are able to confirm that it contributes to the biogenesis of CCVs during infection.

Acknowledgments

We would like to kindly thank Prof Bob Heinzen (Rocky Mountain Laboratories, NIH) for supplying *C. burnetii* expression plasmids, Prof Jenny Stow (University of Queensland) for the GFP-Rab7 plasmid, Prof Craig Roy (Yale School of Medicine, Yale University) for the GFP-Clathrin plasmid, and Prof Jason Mackenzie (Peter Doherty Institute, University of Melbourne) for the GFP-LC3 plasmid. We thank the team at the Biological Optical Microscopy Platform (BOMP, University of Melbourne) and the Monash Micro Imaging platform (MMI, Monash University) who provided invaluable technical expertise and maintenance for the confocal microscopy used in this study. The Australian Genome Research Facility (AGRF) provided sequencing services in Melbourne. We thank the Melbourne Mass Spectrometry and Proteomics Facility of The Bio21 Molecular Science and Biotechnology Institute for access to MS instrumentation.

Author contributions

David R. Thomas (Data curation, Formal analysis, Investigation, Methodology, Supervision, Validation, Writing – original draft, Writing – review & editing), Sarah E. Garnish (Data curation, Formal analysis, Validation, Writing – review & editing), Chen Ai Khoo (Data curation, Investigation, Methodology, Supervision, Writing – review & editing), Bhavna Padmanabhan (Data curation, Investigation, Methodology, Writing – review & editing), Nichollas E. Scott (Methodology, Supervision, Visualization, Writing – review & editing), and Hayley J. Newton (Conceptualization, Data curation, Formal analysis, Funding acquisition, Project administration, Resources, Supervision, Writing – review & editing)

Supplementary data

Supplementary data is available at *FEMSPD Journal* online.

Conflict of interest: None declared.

Funding

This research was supported by the NHMRC Ideas Grant 2010841. N.E.S is supported by an Australian Research Council Future Fellowship (FT200100270) and an ARC Discovery Project Grant (DP210100362).

References

Asai M, Li Y, Newton SM *et al.* Galleria mellonella-intracellular bacteria pathogen infection models: the ins and outs. *FEMS Microbiol Rev* 2023;**47**.

Beare PA, Gilk SD, Larson CL *et al.* Dot/icm type IVB secretion system requirements for Coxiella burnetii growth in human macrophages. *mBio* 2011;**2**:e00175–11.

Beare PA, Heinzen RA. Gene inactivation in Coxiella burnetii. *Methods Mol Biol* 2014;**1197**:329–45.

Beron W, Gutierrez MG, Rabinovitch M *et al.* Coxiella burnetii localizes in a Rab7-labeled compartment with autophagic characteristics. *Infect Immun* 2002;**70**:5816–21.

Buijs SB, Bleeker-Rovers CP, Van Roeden SE *et al.* Still new chronic Q fever cases diagnosed 8 years after a large Q fever outbreak. *Clin Infect Dis* 2021;**73**:1476–83.

Burette M, Allombert J, Lambou K *et al.* Modulation of innate immune signaling by a Coxiella burnetii eukaryotic-like effector protein. *P Natl Acad Sci USA* 2020;**117**:13708–18.

Carey KL, Newton HJ, Luhrmann A *et al.* The Coxiella burnetii Dot/Icm system delivers a unique repertoire of type IV effectors into host cells and is required for intracellular replication. *PLoS Pathog* 2011;**7**:e1002056.

Case EDR, Mahapatra S, Hoffpauir CT *et al.* Primary murine macrophages as a tool for virulence factor discovery in Coxiella burnetii. *Microbiol Spectr* 2022;**10**:e0248421.

Chen C, Banga S, Mertens K *et al.* Large-scale identification and translocation of type IV secretion substrates by Coxiella burnetii. *Proc Natl Acad Sci USA* 2010;**107**:21755–60.

Crabill E, Schofield WB, Newton HJ *et al.* Dot/Icm-translocated proteins important for biogenesis of the coxiella burnetii-containing vacuole identified by screening of an effector mutant sublibrary. *Infect Immun* 2018:**86**.

Dragan AL, Kurten RC, Voth DE. Characterization of early stages of Human alveolar infection by the Q fever agent coxiella burnetii. *Infect Immun* 2019;**87**.

Fielden LF, Moffatt JH, Kang Y *et al.* A farnesylated coxiella burnetii effector forms a multimeric complex at the mitochondrial outer membrane during infection. *Infect Immun* 2017;**85**.

Jaton K, Peter O, Raoult D *et al.* Development of a high throughput PCR to detect coxiella burnetii and its application in a diagnostic laboratory over a 7-year period. *New Microbes New Infect* 2013;**1**:6–12.

Jumper J, Evans R, Pritzel A *et al.* Highly accurate protein structure prediction with AlphaFold. *Nature* 2021;**596**:583–9.

Kelley LA, Mezulis S, Yates CM *et al.* The Phyre2 web portal for protein modeling, prediction and analysis. *Nat Protoc* 2015;**10**:845–58.

Kohler LJ, Reed Sh C, Sarraf SA *et al.* Effector protein Cig2 decreases host tolerance of infection by directing constitutive fusion of autophagosomes with the coxiella-containing vacuole. *mBio* 2016;**7**.

Kong AT, Leprevost FV, Avtonomov DM *et al.* MSFragger: ultrafast and comprehensive peptide identification in mass spectrometry-based proteomics. *Nat Methods* 2017;**14**:513–20.

Kong W, Hui HWH, Peng H *et al.* Dealing with missing values in proteomics data. *Proteomics* 2022;**22**:e2200092.

Kuba M, Neha N, Newton P *et al.* EirA is a novel protein essential for intracellular replication of coxiella burnetii. *Infect Immun* 2020;**8**:e00913–19.

Larson CL, Beare PA, Howe D *et al.* Coxiella burnetii effector protein subverts clathrin-mediated vesicular trafficking for pathogen vacuole biogenesis. *P Natl Acad Sci USA* 2013;**110**:E4770–9.

Larson CL, Beare PA, Voth DE *et al.* Coxiella burnetii effector proteins that localize to the parasitophorous vacuole membrane promote intracellular replication. *Infect Immun* 2015;**83**:661–70.

Larson CL, Pullman W, Beare PA *et al.* Identification of type 4B secretion system substrates that are conserved among Coxiella burnetii genomes and promote intracellular growth. *Microbiol Spectr* 2023;**11**:e0069623.

Larson CL, Sandoz KM, Cockrell DC *et al.* Noncanonical inhibition of mTORC1 by Coxiella burnetii promotes replication within a phagolysosome-like vacuole. *mBio* 2019;**10**.

Latomanski EA, Newton HJ. Interaction between autophagic vesicles and the Coxiella-containing vacuole requires CLTC (clathrin heavy chain). *Autophagy* 2018;**14**:1710–25.

Latomanski EA, Newton P, Khoo CA *et al.* The effector Cig57 hijacks FCHO-mediated vesicular trafficking to facilitate intracellular replication of coxiella burnetii. *PLoS Pathog* 2016;**12**:e1006101.

Lau N, Haeberle AL, O'keeffe BJ *et al.* SopF, a phosphoinositide binding effector, promotes the stability of the nascent Salmonella-containing vacuole. *PLoS Pathog* 2019;**15**:e1007959.

Lau N, Thomas DR, Lee YW *et al.* Perturbation of ATG16L1 function impairs the biogenesis of Salmonella and coxiella replication vacuoles. *Mol Microbiol* 2022;**117**:235–51.

Lifshitz Z, Burstein D, Peeri M *et al.* Computational modeling and experimental validation of the Legionella and Coxiella virulence-related type-IVB secretion signal. *Proc Natl Acad Sci USA* 2013;**110**:E707–15.

Loterio RK, Thomas DR, Andrade W *et al.* Coxiella co-opts the Glutathione Peroxidase 4 to protect the host cell from oxidative stress-induced cell death. *Proc Natl Acad Sci USA* 2023;**120**:e2308752120.

Martinez E, Allombert J, Cantet F *et al.* Coxiella burnetii effector CvpB modulates phosphoinositide metabolism for optimal vacuole development. *Proc Natl Acad Sci USA* 2016;**113**:E3260–9.

Martinez E, Cantet F, Fava L *et al.* Identification of OmpA, a Coxiella burnetii protein involved in host cell invasion, by multi-phenotypic high-content screening. *PLoS Pathog* 2014;**10**:e1004013.

Maurin M, Raoult D. Q fever. *Clin Microbiol Rev* 1999;**12**:518–53.

Metters G, Hemsley C, Norville I *et al.* Identification of essential genes in Coxiella burnetii. *Microb Genom* 2023:**9**.

Newton HJ, Kohler LJ, Mcdonough JA *et al.* A screen of Coxiella burnetii mutants reveals important roles for Dot/Icm effectors and host autophagy in vacuole biogenesis. *PLoS Pathog* 2014;**10**:e1004286.

Newton HJ, Mcdonough JA, Roy CR. Effector protein translocation by the Coxiella burnetii Dot/Icm type IV secretion system requires endocytic maturation of the pathogen-occupied vacuole. *PLoS One* 2013;**8**:e54566.

Newton P, Latomanski EA, Newton HJ. Applying fluorescence resonance energy transfer (FRET) to examine effector translocation efficiency by coxiella burnetii during siRNA silencing. *J Vis Exp* 2016;**113**:54210.

Newton P, Thomas DR, Reed SCO *et al.* Lysosomal degradation products induce Coxiella burnetii virulence. *P Natl Acad Sci USA* 2020;**117**:6801–10.

Norville IH, Hartley MG, Martinez E *et al.* Galleria mellonella as an alternative model of Coxiella burnetii infection. *Microbiology (Reading)* 2014;**160**:1175–81.

Omsland A, Beare PA, Hill J *et al.* Isolation from animal tissue and genetic transformation of coxiella burnetii are facilitated by an improved axenic growth medium. *Appl Environ Microb* 2011;**77**:3720–5.

Padmanabhan B, Fielden LF, Hachani A *et al.* Biogenesis of the spacious coxiella-containing vacuole depends on host transcription factors TFEB and TFE3. *Infect Immun* 2020;**88**.

Rappsilber J, Ishihama Y, Mann M Stop and go extraction tips for matrix-assisted laser desorption/ionization, nanoelectrospray, and LC/MS sample pretreatment in proteomics. *Anal Chem* 2003;**75**:663–70.

Rappsilber J, Mann M, Ishihama Y. Protocol for micro-purification, enrichment, pre-fractionation and storage of peptides for proteomics using StageTips. *Nat Protoc* 2007;**2**:1896–906.

Robi DT, Demissie W, Temteme S. Coxiellosis in livestock: epidemiology, public health significance, and prevalence of Coxiella burnetii infection in Ethiopia. *Vet Med (Auckl)* 2023;**14**:145–58.

Samanta D, Clemente TM, Schuler BE *et al.* Coxiella burnetii Type 4B Secretion system-dependent manipulation of endolysosomal maturation is required for bacterial growth. *PLoS Pathog* 2019;**15**:e1007855.

Sanchez SE, Goodman AG, Omsland A. Metabolic plasticity aids amphotropism of coxiella burnetii. *Infect Immun* 2021;**89**:e0013521.

Schindelin J, Arganda-Carreras I, Frise E *et al.* Fiji: an open-source platform for biological-image analysis. *Nat Methods* 2012;**9**:676–82.

Stirling DR, Swain-Bowden MJ, Lucas AM *et al.* CellProfiler 4: improvements in speed, utility and usability. *BMC Bioinf* 2021;**22**:433.

Tyanova S, Temu T, Sinitcyn P *et al.* The Perseus computational platform for comprehensive analysis of (prote)omics data. *Nat Methods* 2016;**13**:731–40.

Vanderaa C, Gatto L. Revisiting the thorny issue of missing values in single-cell proteomics. *J Proteome Res* 2023;**22**:2775–84.

Van Roeden SE, Wever PC, Kampschreur LM *et al.* Chronic Q fever-related complications and mortality: data from a nationwide cohort. *Clin Microbiol Infect* 2019;**25**:1390–8.

Varadi M, Anyango S, Deshpande M *et al.* AlphaFold Protein Structure Database: massively expanding the structural coverage of protein-sequence space with high-accuracy models. *Nucleic Acids Res* 2022;**50**:D439–44.

Voth DE, Beare PA, Howe D *et al.* The Coxiella burnetii cryptic plasmid is enriched in genes encoding type IV secretion system substrates. *J Bacteriol* 2011;**193**:1493–503.

Wachter S, Larson CL, Virtaneva K *et al.* A survey of two-component systems in Coxiella burnetii reveals redundant regulatory schemes and a requirement for an Atypical PhoBR system in mammalian cell infection. *J Bacteriol* 2023;**205**:e0041622.

Weber MM, Chen C, Rowin K *et al.* Identification of coxiella burnetii type IV secretion substrates required for intracellular replication and coxiella-containing vacuole formation. *J Bacteriol* 2013;**195**:3914–24.

Yang J, Yan R, Roy A *et al.* The I-TASSER Suite: protein structure and function prediction. *Nat Methods* 2015;**12**:7–8.

Received 8 January 2024; **revised** 28 July 2024; **accepted** 13 August 2024